Dynamic CO_2 Adsorption Performance of Internally Cooled Silica-Supported Poly(ethylenimine) Hollow Fiber Sorbents

Yanfang Fan, Ying Labreche, Ryan P. Lively, Christopher W. Jones, and William J. Koros
School of Chemical & Biomolecular Engineering, Georgia Institute of Technology, Atlanta, GA 30332

DOI 10.1002/aic.14615
Published online September 16, 2014 in Wiley Online Library (wileyonlinelibrary.com)

The dynamic adsorption behavior of CO_2 under both nonisothermal and nearly isothermal conditions in silica supported poly(ethylenimine) (PEI) hollow fiber sorbents (Torlon®-S-PEI) is investigated in a rapid temperature swing adsorption (RTSA) process. A maximum CO_2 breakthrough capacity of 1.33 mmol/g-fiber (2.66 mmol/g-silica) is observed when the fibers are actively cooled by flowing cooling water in the fiber bores. Under dry CO_2 adsorption conditions, heat released from the CO_2-amine interaction increases the CO_2 breakthrough capacity by reducing the severity of the diffusion resistance in the supported PEI. This internal resistance can also be alleviated by prehydrating the fiber sorbent with a humid N_2 feed. The CO_2 breakthrough capacity of prehydrated fibers is adversely affected by the release of the adsorption enthalpy (unlike the dry fibers); however, active cooling of the fiber results in a constant CO_2 breakthrough capacity even at high CO_2 delivery rates (i.e., high adsorption enthalpy delivery rates). In full RTSA cycles, a purity of 50% CO_2 is achieved and the adsorption enthalpy recovery rate can reach ~72%. Studies on the cyclic stability of uncooled fiber sorbents in the presence of SO_2 and NO contaminants indicate that exposure to NO at 200 ppm over 120 cycles does not lead to a significant degradation of the sorbents, but SO_2 exposure at a similar high concentration of 200 ppm causes 60% loss in CO_2 breakthrough capacity after 120 cycles. A simple amine reinfusion technique is successfully demonstrated to recover the adsorption capacity in poisoned fiber sorbents after deactivation by exposure to impurities such SO_2. © 2014 American Institute of Chemical Engineers *AIChE J*, 60: 3878–3887, 2014
Keywords: hollow fiber sorbents, poly(ethylenimine), isothermal adsorption, rapid temperature swing adsorption, cyclic stability

Introduction

Although renewable energy technologies are under development, fossil fuels are still the primary source for energy production,[1–3] and will remain so for decades. Fossil fuel consumption continues to overburden the natural environment with billions of tons CO_2 released into the atmosphere every year.[4,5] Global efforts to develop cost-effective carbon dioxide capture technology[5–7] to mitigate the adverse effects of increased CO_2 emission are, therefore, high priorities in the short term. In particular, postcombustion CO_2 capture,[3,8,9] which can be implemented as a retrofit option into existing power plants,[2] has received increasing attention.

Temperature swing adsorption (TSA) processes coupled with amine-oxide hybrid materials[10–16] have been investigated to accelerate the development of efficient CO_2 capture technology from flue gas streams. The high CO_2 adsorption capacity, plus desirable selectivity,[3,14,17] and favorable effects of moisture on adsorption capacities in materials of this type[3,18–21] make them especially attractive. Xu et al.[14] first reported novel "molecular basket" solid sorbents by physically impregnating poly(ethylenimine) (PEI) into silica pores. Other promising amine modified hybrid sorbents, like amine-tethered silica,[10–13,15,16] porous organic polymers with introduction of polyamine groups,[22] have also been reported.

It is important to keep in mind that all the discussed, amine-based chemisorbents have relatively high CO_2 adsorption enthalpies in the range of 50–120 kJ/mol.[16,21,23–25] Although the heat released in a adsorption process is expected to be small in bench-scale experiments,[17] heat management in such TSA processes has to be addressed in practical, large-scale applications.[26–30] Only few studies[17,26–28,30–37] have investigated the role of heat effects on the adsorption performance of solid sorbents. Moreover, considering the substantial energy required to regenerate the chemisorbents, heat integration[38,39] is needed in the entire TSA process to minimize the overall energy penalty. A rapid temperature swing adsorption process (RTSA) with heat integration has been proposed by Lively et al.[39,40] as a potentially economically viable postcombustion CO_2 capture process with the use of polymer-/zeolite-based hollow fiber sorbents. Though the RTSA process, the energetic cost of capturing CO_2 could be dramatically reduced with appropriate heat integration strategies.[39] A full TSA cycle time using fiber sorbents is estimated to be approximately 4 min.

Figure 1 illustrates the cyclic operation process of RTSA. Four beds are operated in different stages, adsorption, heating, sweeping, and cooling, respectively. During the adsorption step, flue gas flows through the shell-side of fiber module, while cooling water is fed through the fiber bores

Correspondence concerning this article should be addressed to W. J. Koros at bill.koros@chbe.gatech.edu or C. W. Jones at cjones@chbe.gatech.edu.

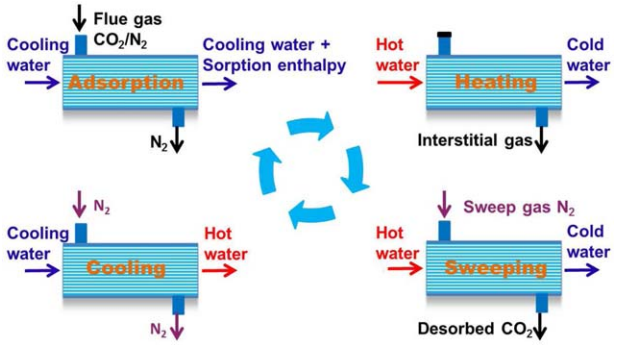

Figure 1. Overview of an RTSA process with heat integration.

[Color figure can be viewed in the online issue, which is available at wileyonlinelibrary.com.]

carrying away the heat of adsorption, which could be potentially reused in a heating stage. After the adsorption step, hot water flowing in the fiber bores heats the fiber and releases CO_2 with the shell-side gas inlet closed. Then, N_2, as a sweeping gas, is fed to the shell-side of the fiber module to push the desorbed CO_2 out of the module. In the specific case of hollow fiber sorbents within an RTSA process, the use of N_2 as the sweep gas instead of steam or pure CO_2 is preferred in future large-scale processes because N_2, derived from cleaned flue gas, will be low cost and can likely perform well in displacing the plug of released CO_2 out of the module without significant axial dispersion/mixing. This desorption mode, which we refer to as plug flow (PF) desorption mode, will result in a purified CO_2 product, as discussed below. In the RTSA process with short cycle times, only a small amount of N_2 is needed in the sweeping stage and the N_2 can potentially be recycled after it displaces CO_2 from the module in a PF manner. The last step of RTSA process is a cooling stage, when cooling water is fed through the fiber bores to reduce the fiber temperature. Heat integration is potentially achieved through this process design by capturing the adsorption enthalpy using the cooling water and heat integrating with other parts of the plant.

In our recent studies, we applied aspects of the RTSA concept, which was originally developed with zeolite adsorbents that require flue gas drying,[40] with cellulose acetate/silica supported amine hollow fiber sorbents (CA-S-PEI)[41–43] to yield a process that combines the favorable aspects of the RTSA approach with the advantages (water tolerance, high CO_2 selectivity, and high capacities) of aminosilica adsorbents. Initially, a new process for synthesis of amine-infused hollow fibers was developed[41,42] and subsequently, the hollow fibers were coated with a low permeability lumen layer, which is necessary to operate the fibers as nanoscopic shell-and-tube heat exchangers, as required for heat integration using the RTSA concept.[39] The new process allows for high dynamic CO_2 capacities in the presence of water and cyclic stability demonstrated over 60 cycles. However, the post-spinning incorporation of the bore side lumen layer can be cumbersome, and a single step, dual layer spinning process would be much more efficient and more readily scalable to commercial scales. To this end, proof-of-concept dual layer poly(amide-imide) (PAI, Torlon®, Solvay Advanced Polymers©)[44] silica hybrid hollow fiber sorbents (Torlon®-S-PEI) were successfully developed in recent work.[45] These fibers are evaluated in depth in this study for the first time. Compared to single layer CA-S-PEI fibers developed by our team,[41] these new fibers have more robust mechanical properties and highly improved chemical stability. In particular, the direct addition of an impermeable lumen layer in the fiber bores during the spinning process simplifies the fiber synthesis process.

In this dynamic study of the Torlon®-S-PEI fiber sorbents, cooling water is flowed in the fiber bores to remove the CO_2 adsorption enthalpy, thereby enabling nearly isothermal adsorption conditions. To understand the effects of preadsorbed water on fiber adsorption performance, both cooled non-prehydrated fibers (with only water picked up from the flue gas in otherwise dry fibers) and prehydrated fibers (fully water saturated) are compared as a function of flue gas flow rates. Fiber adsorption-desorption performance in full RTSA cycles are further evaluated with respect to their potential for internal heat integration, such that the adsorption enthalpy captured from the adsorption step could be reused in the desorption or heating step, in principle.

To achieve widespread deployment of CO_2 capture systems, the practical issues facing CO_2 capture from flue gas such as deactivation by exposure to SO_x and NO_x need to be addressed. Thus, the cyclic CO_2 adsorption performance on exposure to simulated flue gases containing SO_2 and NO in uncooled fiber sorbents is evaluated over 120 RTSA cycles. A technique to recover sorbent adsorption capabilities after deactivation by impurities is demonstrated.

Experiment

Fiber sorbent formation

Silica containing Torlon® and pure Torlon® dual-layer hollow fibers (Torlon®-S) were spun and functionalized using the amine infusion techniques described in our previous work.[41,43] The hollow fibers were a hybrid matrix of PAI, Torlon® (Solvay Advanced Polymers, Alpharetta, GA) and commercial silica (C803, W.R. Grace), with a silica loading of 50 wt % with pure Torlon® as an essentially impermeable lumen layer. The average pore diameter of the silica powder is 18.5–20 nm and the average particle size is 3.8 μm.[41] The fibers are approximately 2000 microns in diameter with a bore diameter of 1000 microns. Poly(ethyleneimine) (PEI) (MW 800, Sigma-Aldrich) was used as the amine source in the postspinning amine infusion step, via application of a 10% PEI solution in methanol.[41] Defects in the lumen layer were further treated by poly(dimethylsiloxane) to enhance the gas and water barrier properties as described in previous studies.[46,47]

CO_2 breakthrough experiments

Hollow fiber modules with a length of 24 in. and diameter of 0.5 in. made from 10 Torlon®-S-PEI fibers were tested in a custom-built RTSA system. The specifics of the RTSA system has been reported in our previous work.[43] T-type hypodermic thermocouples were placed in the middle of the module to measure the temperature profiles of the fiber sorbents during the experiment. The humidified flue gas composition was 13% CO_2, 13% inert tracer He, which has negligible adsorption capacity, 6% H_2O and the balance N_2 (RH 100%). The effluent composition exiting the fiber sorbent module was transiently measured by mass spectrometry (Pfeiffer, Omnistar Quadrupole mass spectrometer QMG

220). All CO_2 adsorption measurements were performed at atmospheric pressure and 35°C unless otherwise noted. The simulated flue gas flow rate ranged from 250 SCCM (standard cubic centimeters per minute, standard is 0°C and 101 kPa) to 650 SCCM and the corresponding gas hourly space velocity varied in a range of 1300–3400 h^{-1}.

The nonadsorbing inert tracer, He, was used to capture the general flow behavior of the fiber sorbent module (i.e., the mean retention time of a nonadsorbing gas) and other nonidealities of the fiber module. Related to this, the breakthrough capacities can be easily calculated by integrating the He signal and CO_2 signal with respect to the time.[48] In uncooled fiber experiments, no water was fed through the fiber bores and the two bore-side ports of the fiber module were sealed using a Swagelok® plug. Adsorption experiments in the cooled fiber were performed at 35°C. Cooling water was pumped through the bores of the fibers in the adsorption process using an Ismatec digital gear pump, which was attached to an in-line water heater (Omega Engineering) that maintained the cooling water temperature at 35°C. The simulated flue gas was fed into the shell side of the hollow fiber module at various flow rates. The cooling water flow rate varied from 70 to 170 mL/min.

Prior to each adsorption experiment, the module was treated at 90°C under flowing N_2 at 300 SCCM for 0.5 h to desorb adventitious CO_2 and water, then cooled down to 35°C and exposed to simulated flue gas. The gas lines downstream of the fiber modules were wrapped in heat tape and held at 120°C to prevent the condensation of water in the gas outlet lines. To study the effects of preadsorbed water in the fibers on the dynamic adsorption behavior (prehydrated fibers), a prehumidification step was used in some runs to ensure the module was saturated with water prior to CO_2 adsorption tests.

CO_2 breakthrough experiments at different adsorption temperatures

CO_2 breakthrough experiments were performed at different adsorption temperatures in both uncooled, non-prehydrated, and prehydrated fibers, where the two bore-side ports of the fiber module were sealed using a Swagelok® plug. Prior to each adsorption experiment, the module was treated at 90°C under flowing N_2 at 300 SCCM for 0.5 h to remove preadsorbed CO_2/H_2O and other impurities (as measured by the downstream mass spectrometer), then cooled to the desired adsorption temperature and subsequently exposed to simulated flue gas at 250 SCCM for 600 s. Various adsorption temperatures were studied in the range of 35–75°C using non-prehydrated fibers. Adsorption temperatures from 35 to 65°C were investigated in prehydrated fibers, due to cabinet temperature limitations.

Rapid temperature swing adsorption/deadsorption using cooling/heating water

In the full cycle RTSA experiment, cooling water was pumped through the bores of the fibers in the adsorption process using an Ismatec digital gear pump, which was attached to the flow from in-line water heater (Omega Engineering) that maintained the cooling water temperature at 35°C. The simulated flue gas was fed into the shell side of the hollow fiber module at 650 SCCM. The cooling water flow rate was maintained at 70 mL/min. In the desorption step, hot water with a temperature of ~110°C was fed to fiber bores to heat the module and then desorb the CO_2. The water line gauge pressure was maintained at 34 kPa by a back pressure regulator.

Cyclic CO_2 adsorption experiment on exposure to SO_2 and NO in uncooled fibers

Dynamic cyclic adsorption/desorption tests were carried out using stainless-steel fiber modules in the RTSA system at 35°C and 1 atm. Two gases containing 200 ppm SO_2 and 200 ppm NO, respectively, mixed with 10% CO_2 and the balance N_2, were used. The fiber module was exposed to these simulated dry flue gases for 10 min. After each adsorption step, the fiber module was heated to 110°C using heat tape and held at 110°C for 25 min to regenerate the fibers in flowing N_2.

Results and Discussion

Effect of flue gas flow rates and preadsorbed water on CO_2 breakthrough capacity in uncooled fibers

Although most of the work reported in the literature has utilized equilibrium CO_2 capacities to evaluate the adsorption capacity of candidate adsorbent materials, the breakthrough capacity, q_b, is a more important parameter in evaluating sorbent utility in a real process. The breakthrough point in this work is defined as the point where CO_2 was detected in the effluent gas. The CO_2 breakthrough capacity, q_b, was determined by integrating the area bounded by He and CO_2 breakthrough curves within the breakthrough point.[48] Here, He acts as the inert tracer to capture the system flow characteristics and CO_2 is the adsorbate of interest.

Figure 2 presents the breakthrough curves and temperature profiles of a non-prehydrated Torlon®-S-PEI module (10 fibers) at various flow rates. The amine loading of these fibers was 5.9 mmol N/g-dry fiber. The "roll-up" of the He tracer signal, which is caused by the replacement of He that is initially filling the fiber pores by CO_2,[48] qualitatively indicates rapid mass transfer within the fiber sorbents. The CO_2 breakthrough front was observed to move faster as flue gas flow rates increased. Concomitantly, the breakthrough capacity, q_b, reduced from 0.82 to 0.68 mmol/g, most likely as a result of internal mass-transfer resistance (Figure 3) associated with diffusion through the silica pores filled with PEI. The CO_2 capacities were determined by normalizing the amount of adsorbed CO_2 by the dry fiber weight. The temperature profiles (Figure 2b) showed that higher gas flow rates of 450 and 650 SCCM gave higher thermal excursions compared to that of the 250 SCCM condition. The thermal waves, which are always observed in nonisothermal adsorption processes, are related to CO_2 adsorption rates, the magnitude of the adsorption enthalpy and the adsorption enthalpy management.[49] As higher flow rates have faster adsorption rates, as indicated by sharper breakthrough fronts, an intense thermal peak was thus observed in the case of the 450 SCCM condition. The 2°C thermal peak reduction observed when increasing the flow rate from 450 to 650 SCCM could be due to the lower adsorption capacity at 650 SCCM, so the total heat released in the adsorption process was reduced.

Figure 4 compares the breakthrough curve and temperature profiles in a non-prehydrated fiber module with those of a prehydrated fiber module (10 fibers) with gas flow rates of 250 SCCM. It was found that CO_2 broke through the bed

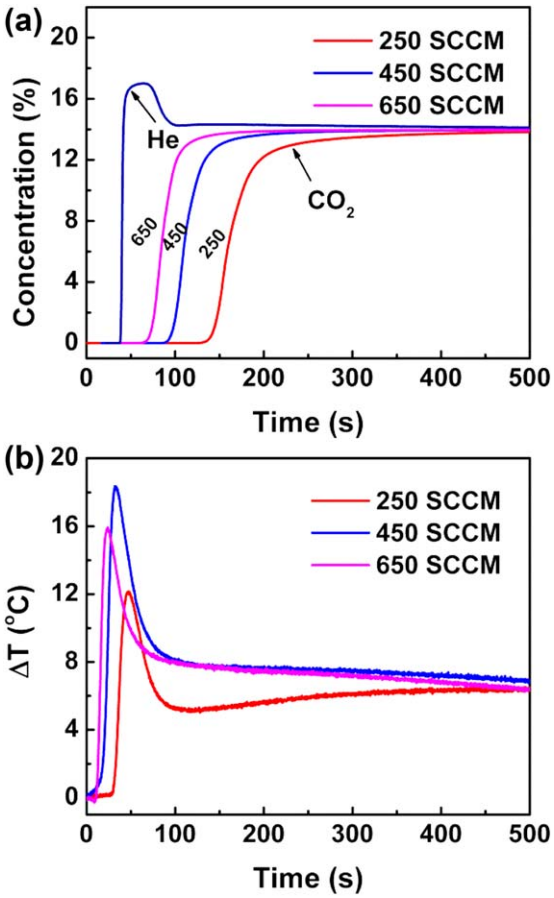

Figure 2. Breakthrough curves (a) and middle-module temperature profiles (b) of non-prehydrated Torlon®-S-PEI at various flow rates with humidified flue gas feed.

ΔT: $T_{fiber} - T_{experiment}$, T_{fiber} is the fiber temperature and $T_{experiment}$ is the experimental temperature of 35°C. [Color figure can be viewed in the online issue, which is available at wileyonlinelibrary.com.]

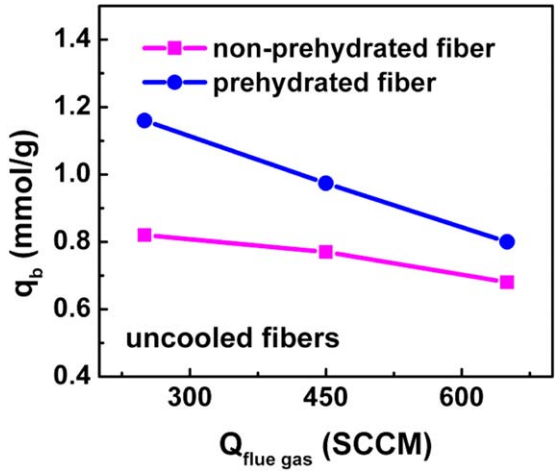

Figure 3. Flow rate effects on adsorption capacity in uncooled, non-prehydrated fibers vs. prehydrated fibers.

[Color figure can be viewed in the online issue, which is available at wileyonlinelibrary.com.]

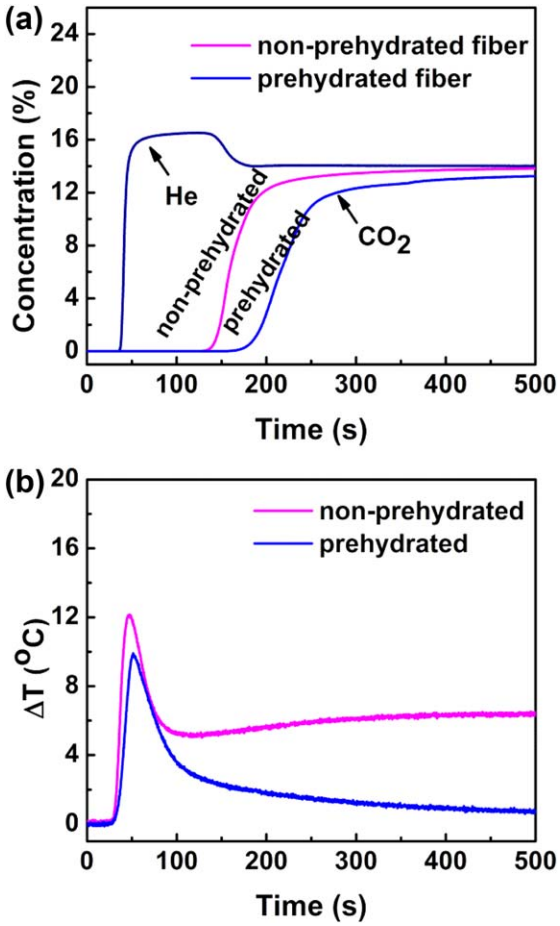

Figure 4. Breakthrough curves (a) and temperature profiles (b) of Torlon®-S-PEI in uncooled non-prehydrated and prehydrated fibers.

ΔT: $T_{fiber} - T_{experiment}$, T_{fiber} is the fiber temperature and $T_{experiment}$ is the experimental temperature of 35°C; $Q_{flue\ gas} = 250$ SCCM. [Color figure can be viewed in the online issue, which is available at wileyonlinelibrary.com.]

40 s later upon prehydrating the fibers and q_b increased from 0.82 to 1.14 mmol/g. For other flow rates such as 450 and 650 SCCM, which are not included in this article, the impacts of preadsorbed water on the breakthrough curves were similar with what was observed at 250 SCCM. This positive effect of water on the adsorption capacity in amine silica hybrid material has been commonly reported in literature.[18–21] Although the increase in CO_2 capacity observed under wet conditions is commonly observed in the literature using amine adsorbents, the cause of this has been attributed to several different factors. It is known from solution chemistry that carbamates can be converted to carbonates/bicarbonates in the presence of water,[50] thus, early studies[3,25,51,52] reported that this may occur in solid adsorbents as well, where a theoretical maximum CO_2/N ratio of 1 may be achieved, yielding a high capacity. However, other explanations for the increase in capacity in the presence of water have been offered in recent studies. Hedin and coworkers[53] found that the formation of ammonium carbamate ion pair as well as hydrogen bonded carbamic acid occurred both in the presence and absence of water, with no evidence for bicarbonate/carbonate. The presence of water was thus suggested to release additional free amine groups to allow more carbamate ions to be produced,[53] thereby showing a positive effect on CO_2

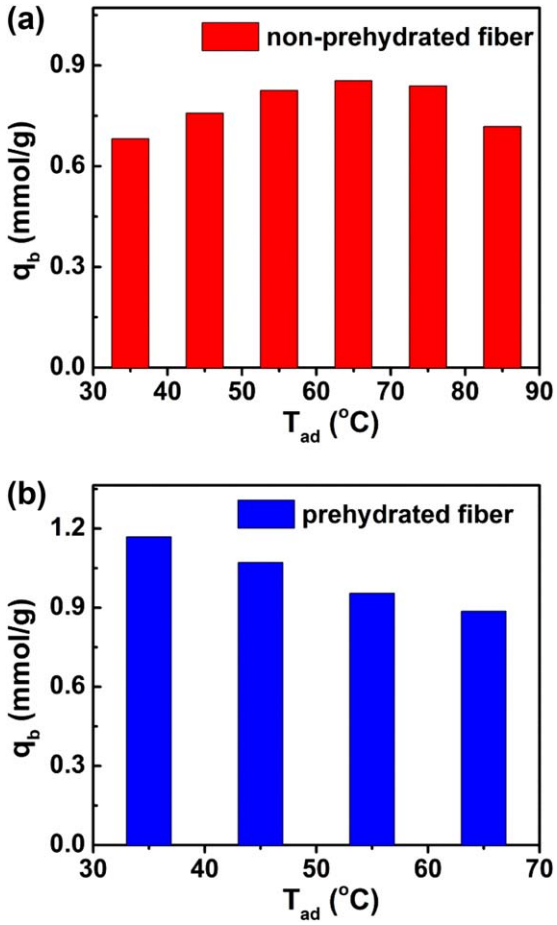

Figure 5. Adsorption temperature T_{ad} effects on adsorption capacity q_b in uncooled non-prehydrated fiber (a) and prehydrated fiber (b).

[Color figure can be viewed in the online issue, which is available at wileyonlinelibrary.com.]

capacity. In a more recent study, Mebane et al.[54] proposed that the adsorption capacity in PEI-loaded silica is most likely related to the availability of diffusive intermediates to transport CO_2, where water molecules in humid CO_2 are favorable for the formation of these intermediates, thereby increasing the adsorption capacity. Thus, the results here show that at all three flue gas flow rates, the preadsorbed water in fibers significantly enhanced the breakthrough capacity q_b (Figure 3), regardless of the root cause.

From the thermal profiles in Figure 4b, the non-prehydrated fibers exhibited more intense thermal waves compared to the prehydrated fiber module. This could be a result of the increase of the total heat capacity of the prehydrated fiber module with the addition of water. Although more heat was released in the prehydrated fiber adsorption process (preadsorbed water enhanced the CO_2 adsorption), a lower thermal peak was observed. In this study, a maximum breakthrough capacity of 1.14 mmol/g was achieved in uncooled prehydrated fibers and the thermal excursion as a result of the exothermic properties of CO_2 adsorption was as high as 18°C.

Effect of adsorption temperature on adsorption performance in uncooled fiber sorbents

The adsorption temperature effects on the uncooled fiber sorbent performance were studied in both non-prehydrated fibers and prehydrated fibers. The breakthrough capacity, q_b, as a function of the adsorption temperature, is demonstrated in Figure 5. In the case of non-prehydrated fibers, a maximum q_b was found at 65°C. This is similar to what has been observed with silica powders whose pores were filled with PEI, where an interplay between the thermodynamics of adsorption and the kinetics of CO_2 diffusion and reaction into the PEI contributed to this unusual phenomenon.[14] As the diffusion limitations were minimized at relatively high temperatures, more amine groups became accessible to the CO_2 molecules, and therefore, q_b exhibited an increasing trend with an increase of adsorption temperature from 35 to 65°C. At temperatures above 65°C, diffusion was fast enough, and thermodynamic properties of adsorption dominated the breakthrough adsorption capacity, leading to a reduction of breakthrough adsorption capacity, q_b, with further increases of the adsorption temperature. Thus, the internal diffusion resistance through PEI-filled pores is likely a dominant factor influencing the dynamic adsorption performance of dry Torlon®-S-PEI fibers.

Interestingly, the CO_2 capacity, q_b, in prehydrated fibers showed a decreasing trend with an increase of adsorption temperature over the entire temperature range. This result suggests that diffusion resistance in PEI, as observed in dry fibers, was not as significant in the prehydrated fibers. This could be due to a "plasticizing effect" from preadsorbed water molecules, which weakens inter or intra molecular hydrogen bonds and dipole–dipole interactions,[55,56] thereby improving PEI dispersity and minimizing internal diffusion limitations. Alternately, if the carbonate/bicarbonate model of CO_2 adsorption is invoked, the presence of water may prevent crosslinks from forming between adjacent amines on different polymer chains, which can occur when ammonium carbamate species are created under dry conditions. Although PEI-based solid adsorbents have been extensively studied, the morphology of the PEI impregnated in the silica pores is still not understood. In recent studies by Wang and Song,[57] a two-layer model was proposed to explain the adsorption behavior in SBA-15 impregnated with PEI. Two layers of PEI in silica pores were postulated in their work, that is, an exposed PEI layer and an inner bulky PEI layer (PEI chain cluster). It was proposed that the CO_2 could easily access the amine groups in the exposed PEI layer, while diffusion limitations had to be overcome for CO_2 to approach the inner bulk PEI layer, where the adsorption behavior was proposed to be similar to pure liquid PEI.[57] In considering the two-layer model in our work, the presence of water may greatly swell the PEI cluster, reducing PEI viscosity, and enable CO_2 to react with more amine groups. Correspondingly, the ratio of exposed PEI to bulk PEI layer was likely increased in prehydrated fibers. Further insights into the nature of the PEI in the silica pores are necessary to achieve a more detailed mechanistic understanding of adsorption and diffusion in PEI impregnated sorbents.

Adsorption capacity in cooled fiber sorbents vs. uncooled fiber sorbents

In a RTSA fiber sorbent process, cooling water is generally fed to the bore-side of the fibers to capture and remove the adsorption enthalpy. This allows the fibers to operate essentially isothermally.[28] Figure 6 compares the breakthrough curves and thermal response in uncooled fiber sorbents with cooled, non-prehydrated Torlon®-S-PEI fibers.

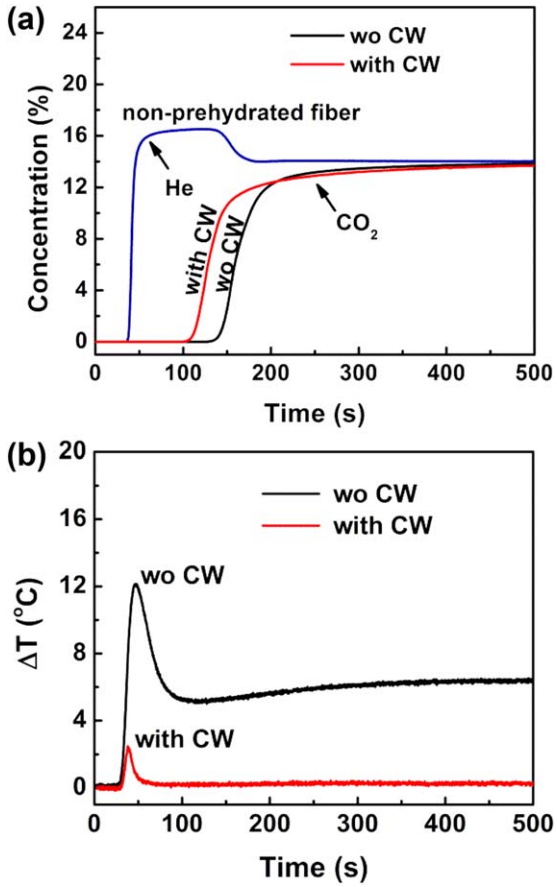

Figure 6. Breakthrough curves (a) and temperature profiles (b) of uncooled vs. cooled non-prehydrated Torlon®-S-PEI.

ΔT: $T_{fiber} - T_{experiment}$, T_{fiber} is the fiber temperature and $T_{experiment}$ is the experimental temperature of 35°C; $Q_{flue\ gas} = 250$ SCCM. [Color figure can be viewed in the online issue, which is available at wileyonlinelibrary.com.]

With flowing cooling water in non-prehydrated fiber bores, it was interestingly found that the CO_2 breakthrough front moved even faster (Figure 6a), accordingly, the breakthrough capacity, q_b, dropped from 0.82 to 0.54 mmol/g, while the thermal wave intensity was dramatically reduced (Figure 6b). This trend indicates that heat effects, which are not favorable in traditional CO_2 adsorbents,[28,33] improved the dynamic adsorption performance in this type of adsorbent. This observation can be understood in light of the unusual temperature dependence of the adsorption capacity in uncooled, non-prehydrated fibers, as discussed earlier. The rise of the fiber temperature as a result of heat released in the adsorption process led to the reduction of CO_2 diffusion limitations in the PEI. Correspondingly, a higher capacity was observed under nonisothermal conditions compared to that in cooled, dry fibers at 35°C.

Additional experiments were performed at various flow rates in cooled, non-prehydrated fibers. The q_b dependence on the gas flow rates $Q_{flue\ gas}$ in cooled fibers was compared with that of the uncooled fibers in Figure 7a. When the flow rate increased from 250 to 650 SCCM, the q_b in cooled, non-prehydrated fibers was consistently lower than that in uncooled fibers. The temperature data in Table 1 demonstrate that flowing cooling water dramatically reduced the thermal peaks observed in the adsorption process. These results suggest that the heat removal yielded a negative impact on the adsorption capacity in the case of low temperature adsorption with non-prehydrated Torlon®-S-PEI fiber sorbents. This may be advantageous for applications where the gas feed is supplied at high temperatures, above 65°C. In that temperature range, the temperature dependence of the adsorption capacity in non-prehydrated fibers illustrates the dominance of thermodynamic properties of adsorption, and heat removal would be beneficial.

To further understand how preadsorbed water in the fibers influences adsorption performance with flowing cooling water, another set of experiments was performed using prehydrated fibers. The comparison of the breakthrough curves in Figure 8a illustrates that a cooled, prehydrated fiber module (10 fibers) has a longer breakthrough time compared to an uncooled fiber module. The breakthrough capacity, q_b, increased from 1.14 to 1.33 mmol/g and the thermal peaks showed a reduction of ~8°C, indicating efficient heat removal from the prehydrated fibers. In the case of prehydrated fibers, both preadsorbed water in the fibers and cooling water flowing in the fiber bores contributed to the improved breakthrough capacity. Preadsorbed water, which

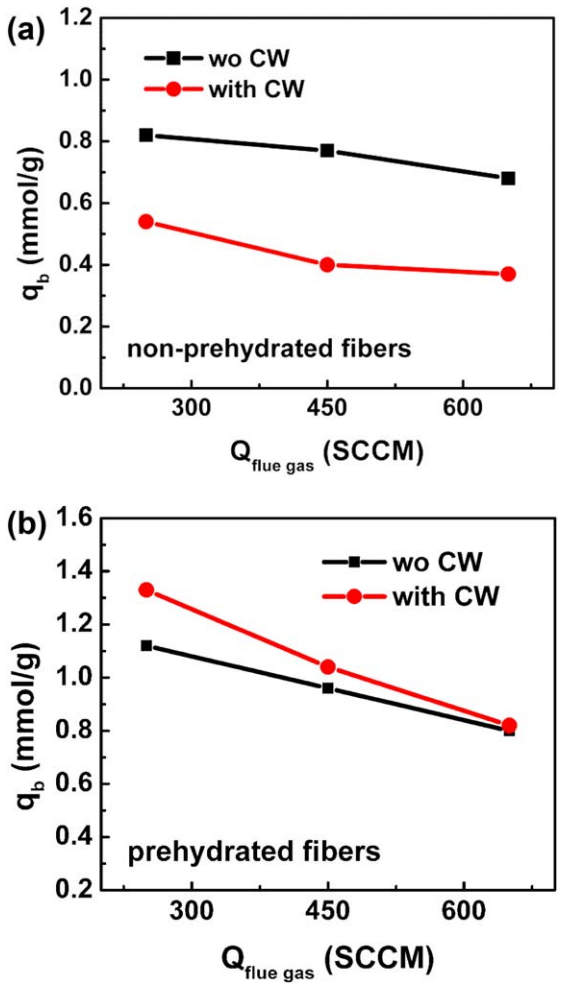

Figure 7. Flow rates effects on adsorption capacity in non-prehydrated fibers (a) and prehydrated fibers (b).

[Color figure can be viewed in the online issue, which is available at wileyonlinelibrary.com.]

Table 1. Cooling Water Effects on Breakthrough Capacity, q_b, and Thermal Excursion in Non-prehydrated Fibers

	Without CW		With CW	
$Q_{flue\ gas}$ (SCCM)	q_b (mmol/g)	ΔT (°C)	q_b (mmol/g)	ΔT (°C)
250	0.82	12	0.54	2.5
450	0.77	18	0.40	2.9
650	0.68	16	0.36	3.8

can partially solvate the bulky PEI in the silica pores, may plasticize the PEI polymer chains by weakening inter and intra molecular hydrogen bonds and dipole–dipole interactions,[55] thereby improving PEI chain segment mobility. Diffusion limitations induced by PEI in the silica pores are expected to be minimized under these conditions. Therefore, the q_b decreased with an increase of adsorption temperature, as shown in Figure 5. Consequently, flowing cooling water that could efficiently remove the heat of adsorption enhanced the breakthrough capacity, q_b (Table 2).

In all the experiments performed above, the cooling water flow rate was maintained at 70 mL/min. To further investigate if the cooling water flow rate was high enough to efficiently remove the adsorption enthalpy, especially at the high gas flow rate (high heat delivery rate), the highest flue gas flow rate of 650 SCCM was used while the water flow rates were varied from 70 to 170 mL/min in a series of experiments. The breakthrough capacity was found to be independent of the cooling water flow rates. This result indicates that the water flow rate of 70 mL/min used in this work can efficiently maintain the fiber sorbent at nearly isothermal conditions. As estimated from the thermal profiles in the adsorption process, the thermal front velocity in the uncooled fiber sorbents was around 0.82 cm/s. The water plug velocity in the fiber bores was 15 cm/s at 70 mL/min, which was much faster than the thermal front velocity. Consequently, a temperature gradient was created between the fiber sorbents and rapidly moving cooling water in the fiber bores so that the thermal front could efficiently transfer heat to a plug of cooling water in the fiber bores.

Flue gas flow rate effects on q_b in cooled, prehydrated fibers vs. those in uncooled, prehydrated fibers are shown in Figure 7b. At three different flow rates, cooled prehydrated fibers exhibited a higher q_b compared to that in uncooled fibers. However, with increasing flue gas flow rate, cooling water effects on q_b in prehydrated fibers were reduced. At 450 SCCM, q_b in the cooled fibers was only slightly higher (~8%) than that in the uncooled fibers. At much higher flow rates of 650 SCCM, q_b in cooled, prehydrated fibers was quite close to that in the uncooled fibers. This is likely associated with high internal mass-transfer resistance in this type of adsorbent.

Lively et al.[28] demonstrated q_b in cooled zeolite-based fiber sorbents was nearly independent of flue gas flow rates, as heat effects were removed. In our work, although thermal excursions were greatly inhibited by active cooling water in fiber bores, q_b in cooled fiber sorbents still showed a decreasing trend with increasing flow rates. Thus, for these fiber sorbents, the breakthrough capacity was correlated with both heat effects and mass-transfer resistance. In contrast to the zeolite-based fiber sorbent, where external mass transfer was the major limiting factor of the adsorption kinetics,[48] internal mass-transfer limitations were postulated to play a

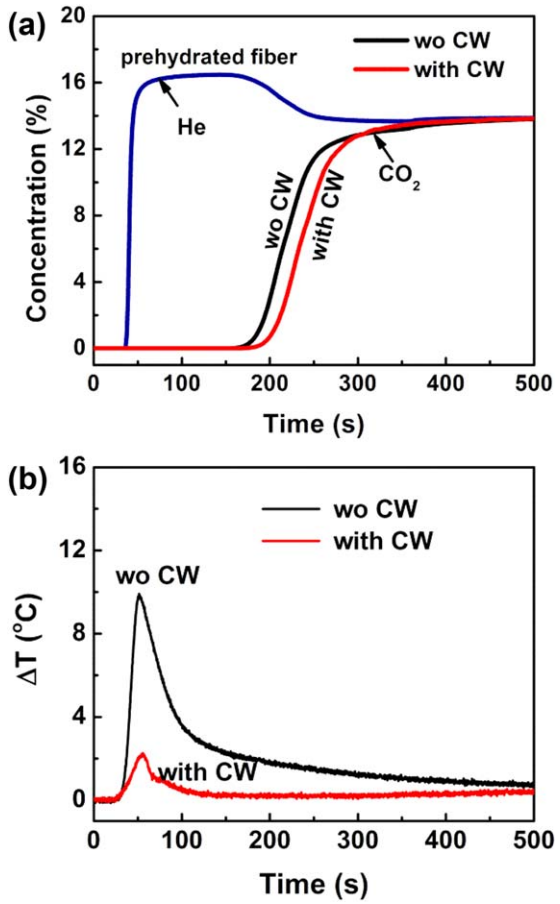

Figure 8. Breakthrough curves (a) and temperature profiles (b) of uncooled vs. cooled prehydrated Torlon®-S-PEI.

ΔT: $T_{fiber} - T_{experiment}$, T_{fiber} is the fiber temperature and $T_{experiment}$ is the experimental temperature of 35°C; $Q_{flue\ gas} = 250$ SCCM. [Color figure can be viewed in the online issue, which is available at wileyonlinelibrary.com.]

key role in the PEI-impregnated silica fiber adsorbents, as evidenced by the temperature dependence of their adsorption capacities, as discussed earlier. In prehydrated fibers, the presence of preadsorbed water led to additional complexity. Water, as a plasticizer, to some extent, reduced the internal diffusion limitation in PEI, thereby enhancing CO_2 transport. In the case of high flue gas flow rates (i.e., much shorter residence times of flue gas in the fiber module), the internal mass transfer was more relevant to kinetic adsorption performance. Thus, q_b in cooled fibers exhibited a decreasing trend with an increase of gas flow rates, even under nearly isothermal conditions. Our results indicate that the internal mass-transfer resistance of the silica-supported amines

Table 2. Cooling Water Effects on Breakthrough Capacity, q_b, and Thermal Excursion in Prehydrated Fibers

	Without CW		With CW	
$Q_{flue\ gas}$ (SCCM)	q_b (mmol/g)	ΔT (°C)	q_b (mmol/g)	ΔT (°C)
250	1.14	100	1.33	2.2
450	0.96	11	1.04	3.4
650	0.80	16	0.82	2.1

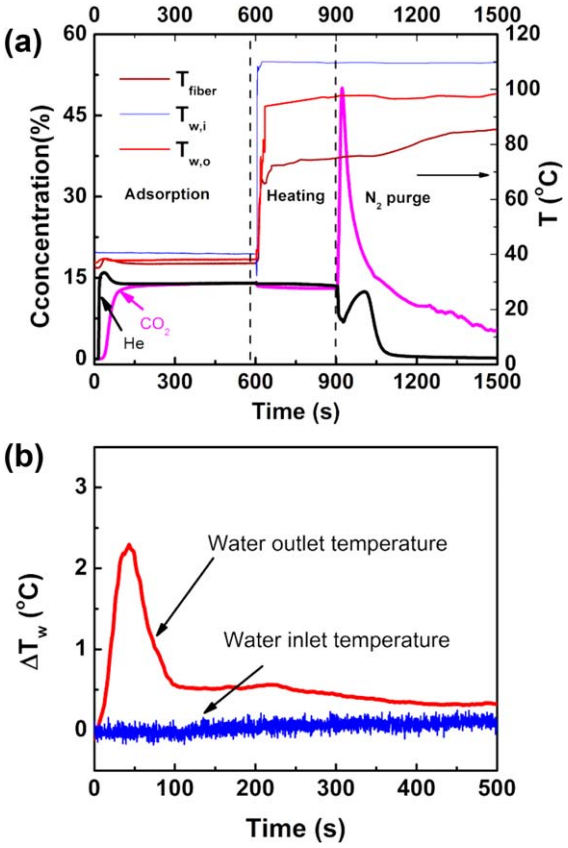

Figure 9. Rapid temperature swing adsorption/desorption cycle in Torlon®-S-PEI fiber sorbents (a); water temperature profiles in deadsorption step (b).

T_{fiber}: fiber sorbent temperature; $T_{w,i}$: water inlet temperature; $T_{w,o}$: water outlet temperature; ΔT_w: the difference between outlet temperature and water inlet temperature. [Color figure can be viewed in the online issue, which is available at wileyonlinelibrary.com.]

should be reduced to improve the overall dynamic performance of amine-loaded hollow fiber sorbents.

In summary, cooling water yields opposite effects on non-prehydrated and prehydrated fibers. Cooled non-prehydrated fibers showed reduced q_b compared to uncooled fibers. In contrast, cooled prehydrated fibers exhibited increased q_b as a result of efficient heat removal. The discrepancy of adsorption behaviors, as mentioned earlier, could mainly be attributed to the plasticizing effect of water molecules preadsorbed in the wet fibers. In practical operation, the fiber module may likely be operated at prehydrated conditions, as complete water removal from fiber sorbents in desorption processes will consume large amounts of energy and will be avoided, if possible. Accordingly, preadsorbed water could greatly benefit the adsorption performance in this type of adsorbent. Further studies are needed to better understand how preadsorbed water in fibers influences the mass transfer and adsorption mechanism in this type of fiber adsorbent.

Full RTSA cycles

A full RTSA cycle was subsequently performed with active heating and cooling in the fiber bores. In the adsorption process, the fiber module (10 fibers) was first saturated with CO_2 by humidified flue gas at 35°C and 1 atm with cooling water fed in the bores. Next, hot water of ~110°C with back pressure of ~34 kPa (gauge pressure) was fed to fiber bores to heat the module for 5 min, with the module inlet and outlet valves closed. Finally, nitrogen was utilized to purge the fiber module to push the desorbed CO_2 out of the module. Figure 9 illustrates the full, non-optimized cycle CO_2 signal and the fiber, water inlet ($T_{w,i}$) and water outlet ($T_{w,o}$) temperature profiles, where the He tracer is included as a reference. The water outlet temperature showed a temperature rise in the adsorption process (Figure 9b), suggesting that the adsorption enthalpy was captured by the flowing cooling water. By integration of the water outlet temperature peaks, the total heat captured was estimated to be approximately 47 kJ/mol-CO_2. Based on adsorption enthalpy of 65 kJ/mol-CO_2 in the PEI impregnated sorbent, a heat capture efficiency of ~72% was achieved in the adsorption step. In the desorption step, a purity of ~50% CO_2 was achieved using a continuous stirred tank (CST) desorption mode, where the fiber module was heated by hot water in the fiber bores with the shell side gas outlet closed. In CST desorption mode, desorbed CO_2 is completely mixed with residual flue gas in the module, and thus product purity is reduced. In the future, plug flow desorption mode (PF) mode[28,29] will be performed and higher purity CO_2 is anticipated to be collected through this approach. In an optimized PF mode, the hot water thermal front moves along the fiber sorbent, and the adsorbed CO_2 is quickly released. When the thermal wave passes the entire fiber length and the majority of the space of the fiber module is filled with concentrated CO_2, N_2 is then used as the sweep gas to push the plug of concentrated CO_2 out of the module. Thus, a CO_2 stream of high purity may be produced in this more optimized desorption process.

Cyclic stability of uncooled fiber sorbents on exposure to SO_2 and NO

The cyclic stability of fiber adsorbents is an important indicator of long-term adsorption performance considering the practical application of adsorbents in a postcombustion CO_2 capture process. SO_x and NO_x impurities in flue gases can react with basic groups in adsorbents to deactivate

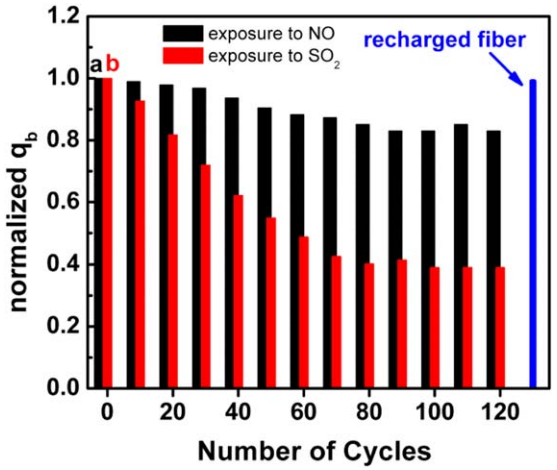

Figure 10. Cyclic stability of Torlon®-S-PEI on exposure to flue gas with 200 ppm SO_2 (a) and 200 ppm NO (b).

[Color figure can be viewed in the online issue, which is available at wileyonlinelibrary.com.]

certain adsorption sites.[51,58–60] Fiber adsorbents of Torlon®-S-PEI were subjected to 120 cyclic rapid adsorption-desorption tests using two different gas mixtures, which include ~200 ppm SO_2, ~200 ppm NO, respectively, besides 10% CO_2 and the balance N_2.

The carbon dioxide capacity, q_b, was compared for 120 cycles, as shown in Figure 10. Only 15% capacity loss was observed in 200 ppm NO. This is likely due to the low NO sorption capacity in aminosilica materials, as demonstrated with powder samples in an earlier study.[60] However, significant degradation of Torlon®-S-PEI was observed in the first 80 cycles on exposure to 200 ppm SO_2, where there was a CO_2 capacity loss of 60% compared to the q_b of the first cycle. Surprisingly, no changes in q_b were observed after 80 cycles. The plateau capacity may perhaps be due to adsorption at remaining isolated amine groups,[61] adsorption at remaining active secondary amine groups,[60] or adsorption as physisorbed CO_2 in the porous silica structure. With the degradation of the sorbents, an increasing amount of surface amine sites irreversibly bind to SO_2; accordingly, the number of isolated amine sites rises progressively, which have been indicated to exhibit much weaker interaction with CO_2.[61] These isolated amine sites are thermally reversible to CO_2. Assuming that SO_2 has a similar gas/amine reaction mechanism as CO_2,[58] isolated amines perhaps bind SO_2 weakly as well, and may have some thermal reversibility. Also, secondary amines have been shown to have a much more reversibility on exposure to SO_2 compared to primary amines.[60] Moreover, the free Si-OH groups on porous silica have some adsorption capability for CO_2 by hydrogen bonding. All these factors may contribute to active adsorbent sites present in the sorbents after SO_2 degradation.

In our previous work, we have demonstrated recharging deactivated CA-S-PEI fibers with fresh PEI could allow for recovery of the CO_2 adsorption capacity (by reinfusing an amine solution into the fiber module).[41,43] The same procedure was applied to the SO_2 deactivated Torlon®-S-PEI fiber module here. It was found that the recharged Torlon®-S-PEI fibers had a similar q_b as the fresh module (Figure 10a). This means that acid-gas deactivated fibers can be recharged in the field by flowing a PEI dissolving (but Torlon® nonsolvent) solution through the modules to remove deactivated PEI and then redepositing fresh PEI in a second solvent/PEI flushing step.

Conclusions

The dynamic adsorption performance in cooled Torlon®-S-PEI fiber adsorbents was compared with that of uncooled fibers in terms of the effects of adsorption heats and preadsorbed water. Heat released in the adsorption process from the exothermic reaction of CO_2 with amines, which is not favorable for traditional adsorbents, increased the capacity in non-prehydrated Torlon®-S-PEI fibers. A distinctive adsorption behavior was found in prehydrated fibers, where a likely water plasticizing effect reduced diffusion limitations in PEI, thus positive effects were observed on q_b by heat removal in prehydrated fibers. This study reveals the important role of moisture in postcombustion CO_2 capture using PEI-impregnated sorbents, solvating and plasticizing PEI chain segments to reduce mass-transfer resistance while also potentially influencing the CO_2/amine reaction mechanism (bicarbonate/carbonate formation). Moreover, the work demonstrated a high breakthrough capacity achieved in approximately 3 min that reached 1.33 mmol/g-fiber (corresponding to 2.66 mmol/g-silica). Aggressive concentrations of 200 ppm SO_2 led to significant degradation of the fiber sorbent, as expected. However, the amine infusion technique can be successfully applied to recover CO_2 capacity in fibers that was lost to SO_2 deactivation.

Acknowledgments

The authors acknowledge the DOE-NETL under contract DE-FE0007804 for financial support. However, any opinions, findings, conclusions, or recommendations expressed herein are those of the author(s) and do not necessarily reflect the views of the DOE.

Literature Cited

1. Nehring R. Traversing the mountaintop: world fossil fuel production to 2050. *Philos Trans R Soc London Ser B*. 2009;364:3067–3079.
2. House KZ, Harvey CF, Aziz MJ, Schrag DP. The energy penalty of post-combustion CO2 capture & storage and its implications for retrofitting the U.S. installed base. *Energy Environ Sci*. 2009;2(2):193–205.
3. Choi S, Drese JH, Jones CW. Adsorbent materials for carbon dioxide capture from large anthropogenic point sources. *ChemSusChem*. 2009;2(9):796–854.
4. Oliver JGJ, Janssens-Maenhout G, Muntean M, Peters JAHW. *Trends in Global CO2 Emissions; 2013 Report*. The Hague: PBL Netherlands Environmental Assessment Agency; Ispra: Joint Research Centre, 2013.
5. Herzog H, Golomb D. Carbon capture and storage from fossil fuel use. *Encyclopedia of Energy*, Elsevier Science, Inc., New York, 2004:277–287.
6. Haszeldine S. Carbon capture and storage: how green can black be? *Science*. 2009;325(5948):1647–1652.
7. Mason JA, Sumida K, Herm ZR, Krishna R, Long JR. Evaluating metal-organic frameworks for post-combustion carbon dioxide capture via temperature swing adsorption. *Energy Environ Sci*. 2011;4(8):3030–3040.
8. Figueroa JD, Fout T, Plasynski S, McIlvried H, Srivastava RD. Advances in CO_2 capture technology—the U.S. Department of Energy's Carbon Sequestration Program. *Int J Greenhouse Gas Control*. 2008;2(1):9–20.
9. Attalla MI, Jackson P, Robinson K. Environmental impacts of post-combustion capture: new insight. *Recent Advances in Post-Combustion CO2 Capture Chemistry*. *ACS Symposium Series*. American Chemical Society, Washington, DC, 2012:207–217.
10. Hicks JC, Drese JH, Fauth DJ, Gray ML, Qi G, Jones CW. Designing adsorbents for CO_2 capture from flue gas-hyperbranched aminosilicas capable of capturing CO_2 reversibly. *J Am Chem Soc*. 2008;130(10):2902–2903.
11. Serna-Guerrero R, Belmabkhout Y, Sayari A. Further investigations of CO_2 capture using triamine-grafted pore-expanded mesoporous silica. *Chem Eng J*. 2010;158(3):513–519.
12. Harlick PJE, Sayari A. Applications of pore-expanded mesoporous silicas. 3. Triamine silane grafting for enhanced CO_2 adsorption. *Ind Eng Chem Res*. 2006;45(9):3248–3255.
13. Hedin N, Andersson L, Bergström L, Yan J. Adsorbents for the post-combustion capture of CO_2 using rapid temperature swing or vacuum swing adsorption. *Appl Energy*. 2013;104:418–433.
14. Xu X, Song C, Andresen JM, Miller BG, Scaroni AW. Novel polyethylenimine-modified mesoporous molecular sieve of MCM-41 type as high-capacity adsorbent for CO_2 capture. *Energy Fuels*. 2002;16(6):1463–1469.
15. Khatri RA, Chuang SSC, Soong Y, Gray M. Carbon dioxide capture by diamine-grafted SBA-15: a combined Fourier transform infrared and mass spectrometry study. *Ind Eng Chem Res*. 2005;44(10):3702–3708.
16. Leal O, Bolívar C, Ovalles C, García JJ, Espidel Y. Reversible adsorption of carbon dioxide on amine surface-bonded silica gel. *Inorg Chim Acta*. 1995;240(1–2):183–189.
17. Bollini P, Brunelli NA, Didas SA, Jones CW. Dynamics of CO_2 adsorption on amine adsorbents. 1. Impact of heat effects. *Ind Eng Chem Res*. 2012;51(46):15145–15152.
18. Huang HY, Yang RT, Chinn D, Munson CL. Amine-grafted MCM-48 and silica xerogel as superior sorbents for acidic gas removal from natural gas. *Ind Eng Chem Res*. 2002;42(12):2427–2433.

19. Franchi RS, Harlick PJE, Sayari A. Applications of pore-expanded mesoporous silica. 2. Development of a high-capacity, water-tolerant adsorbent for CO_2. *Ind Eng Chem Res.* 2005;44(21):8007–8013.
20. Serna-Guerrero R, Da'na E, Sayari A. New insights into the interactions of CO_2 with amine-functionalized silica. *Ind Eng Chem Res.* 2008;47(23):9406–9412.
21. Belmabkhout Y, Sayari A. Effect of pore expansion and amine functionalization of mesoporous silica on CO_2 adsorption over a wide range of conditions. *Adsorption.* 2009;15(3):318–328.
22. Lu W, Sculley JP, Yuan D, Krishna R, Wei Z, Zhou HC. Polyamine-tethered porous polymer networks for carbon dioxide capture from flue gas. *Angew Chem Int Ed.* 2012;51(30):7480–7484.
23. Knowles GP, Delaney SW, Chaffee AL. Diethylenetriamine[propyl(silyl)]-functionalized (DT) mesoporous silicas as CO_2 adsorbents. *Ind Eng Chem Res.* 2006;45(8):2626–2633.
24. Knöfel C, Descarpentries J, Benzaouia A, Zelenak V, Mornet S, LIwellyn PL, Hornebecq V. Functionalised micro-/mesoporous silica for the adsorption of carbon dioxide. *Microporous Mesoporous Mater.* 2007;99(1–2):79–85.
25. Bollini P, Didas SA, Jones CW. Amine-oxide hybrid materials for acid gas separations. *J Mater Chem.* 2011;21(39):15100–15120.
26. Sircar S, Kumar R, Anselmo KJ. Effects of column nonisothermality or nonadiabaticity on the adsorption breakthrough curves. *Ind Eng Chem Process Des Dev.* 1983;22(1):10–15.
27. Lee L-K, Ruthven DM. Analysis of thermal effects in adsorption rate measurements. *J Chem Soc Faraday Trans 1.* 1979;75:2406–2422.
28. Lively RP, Chance RR, Mysona JA, Babu V, Deckman H, Leta D, Thomann H, Koros WJ. CO_2 sorption and desorption performance of thermally cycled hollow fiber sorbents. *Int J Greenhouse Gas Control.* 2012;10:285–294.
29. Rezaei F, Subramanian S, Kalyanaraman J, Lively RP, Kawajiri Y, Realff MJ. Modeling of rapid temperature swing adsorption using hollow fiber sorbents. *Chem Eng Sci.* 2014;113:62–76.
30. Pirngruber GD, Guillou F, Gomez A, Clausse M. A theoretical analysis of the energy consumption of post-combustion CO_2 capture processes by temperature swing adsorption using solid sorbents. *Int J Greenhouse Gas Control.* 2013;14:74–83.
31. Farooq S, Hassan MM, Ruthven DM. Heat effects in pressure swing adsorption systems. *Chem Eng Sci.* 1988;43(5):1017–1031.
32. Hwang KS, Jun JH, Lee WK. Fixed-bed adsorption for bulk component system. Non-equilibrium, non-isothermal and non-adiabatic model. *Chem Eng Sci.* 1995;50(5):813–825.
33. Farooq S, Ruthven DM. Heat effects in adsorption column dynamics. 1. Comparison of one- and two-dimensional models. *Ind Eng Chem Res.* 1990;29(6):1076–1084.
34. Farooq S, Ruthven DM. Heat effects in adsorption column dynamics. 2. Experimental validation of the one-dimensional model. *Ind Eng Chem Res.* 1990;29(6):1084–1090.
35. Menard D, Py X, Mazet N. Activated carbon monolith of high thermal conductivity for adsorption processes improvement: part A: adsorption step. *Chem Eng Process: Process Intensif.* 2005;44(9):1029–1038.
36. Rezaei F, Grahn M. Thermal management of structured adsorbents in CO_2 capture processes. *Ind Eng Chem Res.* 2012;51(10):4025–4034.
37. Kim JN, Chue KT, Kim KI, Cho SH, Kim JD. Non-isothermal adsorption of nitrogen-carbon dioxide mixture in a fixed bed of zeolite-X. *J Chem Eng Jpn.* 1994;27(1):45–51.
38. Kim K, Son Y, Lee WB, Lee KS. Moving bed adsorption process with internal heat integration for carbon dioxide capture. *Int J Greenhouse Gas Control.* 2013;17:13–24.
39. Lively RP, Chance RR, Koros WJ. Enabling low-cost CO_2 capture via heat integration. *Ind Eng Chem Res.* 2010;49(16):7550–7562.
40. Lively RP, Chance RR, Kelley BT, Deckman H, Drese J, Jones CW, Koros WJ. Hollow fiber adsorbents for CO_2 removal from flue gas. *Ind Eng Chem Res.* 2009;48(15):7314–7324.
41. Labreche Y, Lively RP, Rezaei F, Chen G, Jones CW, Koros WJ. Post-spinning infusion of poly(ethyleneimine) into polymer/silica hollow fiber sorbents for carbon dioxide capture. *Chem Eng J.* 2013;221:166–175.
42. Rezaei F, Lively RP, Labreche Y, Chen G, Fan Y, Koros WJ, Jones CW. Aminosilane-grafted polymer/silica hollow fiber adsorbents for CO_2 capture from flue gas. *ACS Appl Mater Interfaces.* 2013;5(9):3921–3931.
43. Fan Y, Lively RP, Labreche Y, Rezaei F, Koros WJ, Jones CW. Evaluation of CO_2 adsorption dynamics of polymer/silica supported poly(ethylenimine) hollow fiber sorbents in rapid temperature swing adsorption. *Int J Greenhouse Gas Control.* 2014;21:61–71.
44. Robertson GP, Guiver MD, Yoshikawa M, Brownstein S. Structural determination of Torlon® 4000T polyamide–imide by NMR spectroscopy. *Polymer.* 2004;45(4):1111–1117.
45. Labreche Y, Fan Y, Lively RP, Rezaei F, Jones CW, Koros WJ. Dual layer spinning with lumen layer containing PAI/Silica/PEI hollow fiber sorbent for CO2 separation by rapid temperature swing adsorption. *2014 AICHE Spring Meeting*. New Orleans, LA, 2014.
46. Kosuri MR, Koros WJ. Defect-free asymmetric hollow fiber membranes from Torlon®, a polyamide–imide polymer, for high-pressure CO_2 separations. *J Membr Sci.* 2008;320(1–2):65–72.
47. Ekiner OM, Kulkarni SS. Process for making hollow fiber mixed matrix membranes. US Patent 6663805. 2003.
48. Lively RP, Leta DP, DeRites BA, Chance RR, Koros WJ. Hollow fiber adsorbents for CO_2 capture: kinetic sorption performance. *Chem Eng J.* 2011;171(3):801–810.
49. Ruthven DM. *Principles of Adsorption and Adsorption Processes.* New York: Wiley, 1984.
50. Danckwerts PV. The reaction of CO_2 with ethanolamines. *Chem Eng Sci.* 1979;34(4):443–446.
51. Khatri RA, Chuang SSC, Soong Y, Gray M. Thermal and chemical stability of regenerable solid amine sorbent for CO_2 capture. *Energy Fuels.* 2006;20(4):1514–1520.
52. Chang ACC, Chuang SSC, Gray M, Soong Y. In-situ infrared study of CO_2 adsorption on SBA-15 grafted with γ-(aminopropyl)triethoxysilane. *Energy Fuels.* 2003;17(2):468–473.
53. Bacsik ZN, Ahlsten N, Ziadi A, Zhao GY, Garcia-Bennett A, Artin-Matyte B, Hedin N. Mechanisms and kinetics for sorption of CO_2 on bicontinuous mesoporous silica modified with n-propylamine. *Langmuir.* 2011;27(17):11118–11128.
54. Mebane DS, Kress JD, Storlie CB, Fauth DJ, Gray ML, Li K. Transport, zwitterions, and the role of water for CO_2 adsorption in mesoporous silica-supported amine sorbents. *J Phys Chem C.* 2013;117(50):26617–26627.
55. Matveev YI, Grinberg VY, Tolstoguzov VB. The plasticizing effect of water on proteins, polysaccharides and their mixtures. Glassy state of biopolymers, food and seeds. *Food Hydrocoll.* 2000;14(5):425–437.
56. Gontard N, Guilbert S, Cuq JL. Water and glycerol as plasticizers affect mechanical and water vapor barrier properties of an edible wheat gluten film. *J Food Sci.* 1993;58(1):206–211.
57. Wang X, Song C. Temperature-programmed desorption of CO_2 from polyethylenimine-loaded SBA-15 as molecular basket sorbents. *Catal Today.* 2012;194(1):44–52.
58. Diaf A, Garcia JL, Beckman EJ. Thermally reversible polymeric sorbents for acid gases: CO_2, SO_2, and NO_x. *J Appl Polym Sci.* 1994;53(7):857–875.
59. Deng H, Yi H, Tang X, Liu H, Zhou X. Interactive effect for simultaneous removal of SO_2, NO, and CO_2 in flue gas on ion exchanged zeolites. *Ind Eng Chem Res.* 2013;52(20):6778–6784.
60. Rezaei F, Jones CW. Stability of supported amine adsorbents to SO_2 and NO_x in post combustion CO_2 capture. 1. Single-component adsorption. *Ind Eng Chem Res.* 2013;52(34):12192–12201.
61. Srikanth CS, Chuang SSC. Infrared study of strongly and weakly adsorbed CO_2 on fresh and oxidatively degraded amine sorbents. *J Phys Chem C.* 2013;117(18):9196–9205.

Manuscript received June 4, 2014, and revision received Aug. 25, 2014.